Topic: Degenerate Fermi gas.

* We know the Fermi-Dirac distribution
* We know why the released energy after turning off the trap is not $3k_BT$ per particle in a degenerate Fermi gas

1. The Fermi-Dirac distribution

We know that the probability to find a single-particle state to be occupied is given by

$$f(\varepsilon) = \frac{1}{e^{(\varepsilon-\mu)\beta}+1},$$

where $\beta = \frac{1}{k_BT}$ and μ is defined via

$$N = \sum_i f(\varepsilon_i) = \int d\varepsilon\, D(\varepsilon) f(\varepsilon)$$

where $D(E)$ is the density of states at energy E.

Exercise: Derive $f(\varepsilon)$ under the assumptions

(i) $P_N(\varepsilon) = \frac{e^{-E\beta}}{\sum_\alpha e^{-E_\alpha\beta}}$: The probability to find an N-particle state α in a thermal ensemble

(ii) Every single-particle state i is occupied maximally once.

(iii) we $\mu = F_N - F_{N-1}$ with $F_N = -\frac{1}{\beta}\log\sum_\alpha e^{-E_\alpha\beta}$

(iv) The probability $f(\varepsilon)$ does not depend on N for $N\to\infty$.

2. The free electron gas

Let us illustrate the consequences of the Fermi-Dirac distribution on the example of the free electron gas.

$$\varepsilon(k) = \frac{\hbar^2 k^2}{2m}$$

$$\Rightarrow \int \frac{dk}{(2\pi)^d} = \frac{A_d}{(2\pi)^d} \int_0^\infty dk\, k^{d-1} \Rightarrow D(E) = \begin{cases} \frac{1}{4\pi^2}\left(\frac{2m}{\hbar^2}\right)^{3/2} \varepsilon^{1/2} & d=3 \\ \frac{m}{2\pi\hbar^2} & d=2 \\ \frac{1}{2\pi\hbar}\sqrt{\frac{m}{2}}\,\varepsilon^{-1/2} & d=1 \end{cases}$$

$$d\varepsilon = \frac{d\varepsilon}{dk}dk = \frac{\hbar^2 k}{m}dk$$

$$\Rightarrow dk = \frac{m}{\hbar^2 k}d\varepsilon = \sqrt{\frac{m}{2\hbar^2}}\,\varepsilon^{-1/2}d\varepsilon$$

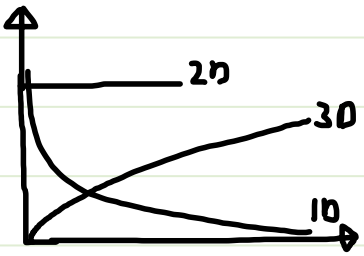

2.1 Fermi energy, p, E_{gs} (3D)

•) $\frac{1}{8\pi^3}\frac{4\pi}{3}k_F^3 = n \Rightarrow k_F = (6\pi^2 n)^{1/3}$

$$\Rightarrow E_F = \frac{\hbar^2(6\pi^2 n)^{2/3}}{2m}$$

→ ~ 4×10^4 K in solids

→ 10^{-7} K in CA

$$v_F = \frac{\hbar}{m}k_F$$

→ 10^6 $\frac{m}{s}$

→ 1 $\frac{cm}{s}$

a) $E_{gs} = \int d\varepsilon D(\varepsilon)\,\varepsilon\,\Theta(\varepsilon_F - \varepsilon) = \frac{3}{5} N\varepsilon_F$

b) $P = -\left.\frac{\partial F}{\partial V}\right|_N = -\frac{\partial}{\partial V}\frac{3}{5}\frac{\hbar^2}{2m}\left(6\pi^2\frac{N}{V}\right)^{2/3} = \frac{2}{3}\frac{3}{5}N\varepsilon_F$

$$\Rightarrow \quad P = \frac{2}{5} N\varepsilon_F$$

2.2 Fermi gas in a harmonic trap

We want to take the harmonic confinement into account.

$$V(\vec{x}) = \sum_{i=1}^{3} \frac{1}{2} m\omega_i^2 x_i^2$$

The energies are given by

$$E_{n_1 n_2 n_3} = \sum_{i=1}^{3} \hbar\omega_i\left(n_i + \frac{1}{2}\right)$$

We calculate the density of states $D(E)$ by counting the number of states in an energy surface of radius $\varepsilon = \varepsilon_x + \varepsilon_y + \varepsilon_z$ where $\varepsilon_\alpha = \hbar\omega_\alpha n_\alpha$

$$G(\varepsilon) = \frac{1}{\hbar^3\omega_x\omega_y\omega_z}\int_0^{\varepsilon} d\varepsilon_x \int_0^{\varepsilon-\varepsilon_x} d\varepsilon_y \int_0^{\varepsilon-\varepsilon_x-\varepsilon_y} d\varepsilon_z = \frac{\varepsilon^3}{6\,(\hbar\bar{\omega})^3}$$

with $\bar{\omega} = (\omega_1\omega_2\omega_3)^{1/3}$

$$\Rightarrow D(\varepsilon) = \frac{d G(\varepsilon)}{d\varepsilon} = \frac{\varepsilon^2}{2(\hbar\bar{\omega})^3}$$

We can now calculate the Fermi energy, pressure, etc.:

•) $$N = \int_0^{E_F} d\varepsilon\, D(E) = \frac{1}{2(\hbar\bar{\omega})^3} \int_0^{\varepsilon_F} d\varepsilon\, \varepsilon^2 = \frac{1}{6(\hbar\bar{\omega})^3} E_F^3$$

$$\Rightarrow E_F = (6N)^{1/3} \hbar\bar{\omega} \longrightarrow 10^{-7}\,\mathrm{K}$$

•) $$U = \int_0^{E_F} d\varepsilon\, \varepsilon\, D(\varepsilon) = \frac{1}{2(\hbar\bar{\omega})^3} \int d\varepsilon\, \varepsilon^3 = \frac{1}{8(\hbar\bar{\omega})^3} \varepsilon_F^4$$

$$= \frac{1}{8}(6N)^{4/3} \hbar\bar{\omega} = \frac{3}{4} N E_F$$

Let us compare this to $u = \frac{U}{N} = 3k_B T$ in a classical gas.

Trapped Fermi gases

D. A. Butts[1] and D. S. Rokhsar[1,2]
[1]*Department of Physics, University of California, Berkeley, California 94720-7300*
[2]*Volen Center for Complex Systems, Brandeis University, Waltham, Massachusetts 02254*
(Received 9 December 1996)

We study the properties of a spin-polarized Fermi gas in a harmonic trap, using the semiclassical (Thomas-Fermi) approximation. Universal forms for the spatial and momentum distributions are calculated, and the results compared with the corresponding properties of a dilute Bose gas. [S1050-2947(97)05306-7]

PACS number(s): 03.75.Fi, 05.30.Fk

I. INTRODUCTION

Trapped degenerate atomic gases provide exciting opportunities for the manipulation and quantitative study of quantum statistical effects, such as the strikingly direct observation of Bose-Einstein condensation [1–3]. Although perhaps not as dramatic as the phase transition associated with bosons, the behavior of trapped Fermi gases also merits attention, both as a degenerate quantum system in its own right and as a possible precursor to a paired Fermi condensate at lower temperatures [4].

The ideal Fermi gas is an old and well-understood problem; there are many familiar systems where the noninteracting Fermi gas is a good zeroth-order approximation. Unlike electrons in atoms and metals, and nucleons in nuclei, however, the trapped atomic gases of Refs. [1–3] are dilute. The effects of predominantly short-ranged atom-atom interactions are therefore weak. For dilute, spin-polarized Fermi gases, the s-wave scattering amplitude (which would dominate the behavior of a comparable gas of distinguishable particles) vanishes due to the antisymmetry of the many-fermion wave function. The next leading order, p-wave scattering is small at low energy, and can be neglected [5].

At low temperatures, both the Bose [6] and Fermi [7] gases are expanded relative to a classical gas at the same temperature. For fermions, however, this effect is due to the Pauli exclusion principle rather than atom-atom interactions. While in the Bose case a phase transition separates the degenerate and classical regimes, a trapped Fermi gas undergoes a gradual crossover between the classical limit and the compact Fermi sea.

Harmonic traps provide a particularly simple realization of the confined Fermi system. In this paper we calculate the chemical potential, specific heat, and spatial and momentum distributions of a harmonically trapped, spin-polarized, ideal Fermi gas. These properties are described by universal scaling functions for any number of particles. We show that the observation of the spatial distribution of the trapped cloud would provide an explicit visualization of a real-space ''Fermi sea.''

II. DENSITY OF STATES

Consider N spin-polarized fermions of mass M moving in an azimuthally symmetric harmonic potential, with a single-particle Hamiltonian

$$\mathcal{H}(\mathbf{r},\mathbf{p})=\frac{1}{2M}[p_x^2+p_y^2+p_z^2]+\frac{M\omega_r^2}{2}[x^2+y^2+\lambda^2 z^2], \tag{1}$$

where ω_r and $\omega_z=\lambda\omega_r$ are the trap frequencies in the radial and axial directions, respectively. The single-particle levels of Eq. (1) are familiar:

$$\epsilon_{n_x,n_y,n_z}=\hbar\omega_r[n_x+n_y+\lambda n_z], \tag{2}$$

where n_x, n_y, and n_z are non-negative integers, and the zero-point energy has been suppressed. In recent experiments with trapped atomic gases, thermal energies far exceed the level spacing ($k_BT\gg\hbar\omega$). We may, therefore, replace this discrete single-particle spectrum with a continuum whose density of states is

$$g(\epsilon)=\frac{\epsilon^2}{2\lambda(\hbar\omega_r)^3}. \tag{3}$$

III. ENERGY AND LENGTH SCALES

The chemical potential $\mu(T,N)$ is given implicitly by

$$N=\int\frac{g(\epsilon)d\epsilon}{e^{\beta(\epsilon-\mu)}+1}. \tag{4}$$

At zero temperature the Fermi-Dirac occupation factor is unity for energies less than the Fermi energy $E_F\equiv\mu(T=0,N)$, and zero otherwise. A straightforward integration of Eq. (4) then gives [7]

$$E_F=\hbar\omega_r[6\lambda N]^{1/3}, \tag{5}$$

which sets the characteristic energy of the atomic cloud.

The characteristic size of the trapped degenerate Fermi gas R_F is given by the excursion of a classical particle with total energy E_F in the trap potential [7]:

$$R_F\equiv[2E_F/M\omega_r^2]^{1/2}=(48N\lambda)^{1/6}\sigma_r, \tag{6}$$

where $\sigma_r=(\hbar/M\omega_r)^{1/2}$ is the radial width of the Gaussian ground state of the trap. For large N, the width of the degenerate Fermi cloud is much greater than the quantum length σ_r, and the Fermi energy is much greater than the level spacing of the trap, due to the Pauli exclusion induced ''repulsion'' between fermions.

Similarly, we may define a characteristic wave number K_F, which is determined by the momentum of a free particle of energy E_F:

$$K_F \equiv [2ME_F/\hbar^2]^{1/2} = (48N\lambda)^{1/6}\sigma_r^{-1}, \tag{7}$$

$$= (48N\lambda/R_F^3)^{1/3}. \tag{8}$$

From Eq. (8) we see that K_F is roughly the reciprocal of the typical interparticle spacing in the gas.

As an example, consider spin-polarized ^{6}Li. The radial frequency of this fermionic isotope of lithium in the trap of Ref. [1] would be $\omega_r = 3800\ \mathrm{sec}^{-1}$. The level spacing $\hbar\omega_r$ then corresponds to 30 nK, and the characteristic ground-state length σ_r is 1.6 μm. The trap has an intrinsic axial-radial ratio $\lambda = \sqrt{8}$. For $N = 10^5$ atoms, the radius R_F is 25 μm; the typical interparticle spacing $1/K_F$ is 100 nm. The Fermi temperature for this gas would be 3.5 μK, a hundred times greater than the level spacing. A back-of-the-envelope calculation confirms that the shift in E_F due to interactions can be neglected [5].

IV. CHEMICAL POTENTIAL AND SPECIFIC HEAT VS TEMPERATURE

For general temperature, the chemical potential μ must be determined numerically using Eq. (4). We can find analytic expressions, however, in the limits of high and low temperature. For low temperature ($k_BT \ll E_F$) the chemical potential is given by the Sommerfeld expansion

$$\mu(T,N) = E_F\left[1 - \frac{\pi^2}{3}\left(\frac{k_BT}{E_F}\right)^2\right]. \tag{9}$$

The third- and higher-order terms in the Sommerfeld series vanish since the density of states is a quadratic function of energy. At high temperatures (i.e., in the classical limit $k_BT \gg E_F$), we find

$$\mu(T,N) = -k_BT\ \ln\left[6\left(\frac{k_BT}{E_F}\right)^3\right]. \tag{10}$$

Numerical results for $\mu(T)/E_F$ are compared with these two limiting forms in Fig. 1. Evidently the low-temperature approximation is quantitatively accurate below $k_BT/E_F \sim 0.55$, while the classical expression holds for higher temperatures.

In Eqs. (9) and (10), the particle number N enters $\mu(T,N)$ only through the Fermi energy E_F. This result holds generally for all temperatures, as can be seen by casting Eq. (4) in dimensionless form by scaling E, μ, and $1/\beta$ by E_F. (The same conclusion holds for any density of states of the form $g(\epsilon) = A\epsilon^b$, for constant A, b.) Figure 1 is therefore a universal curve for harmonically trapped Fermi gases containing any number of particles.

The specific heat per particle of the trapped Fermi gas [8] is defined as $C_N \equiv 1/N\partial E/\partial T|_N$, where $E(T,N)$ is total internal energy of the gas. As seen in Fig. 2, C_N is a monotonic function of temperature. For low temperatures the specific heat per particle is $\pi^2 k_B(k_BT/E_F)$; as we approach the equipartition limit at high temperature $C_N = 3Nk_B$.

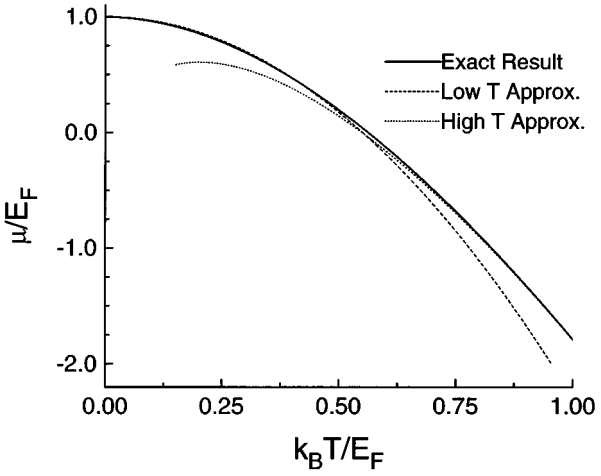

FIG. 1. Chemical potential vs temperature. Both axes are scaled by the Fermi energy, which results in a universal curve that applies to all harmonically trapped Fermi gases.

V. SEMICLASSICAL (THOMAS-FERMI) APPROXIMATION

Since the exact eigenstates of the harmonic potential are well known, the properties of a harmonically trapped ideal gas can, in principle, be found directly by summing over these states. It is useful, however, to have approximate forms for various observables that can be computed directly in the large N limit, where the exact sums become unwieldy.

In the ''semiclassical'' or Thomas-Fermi approximation [9], the state of each atom is labeled by a position $\mathbf{r}$ and a wave vector $\mathbf{k}$, which can be viewed as the centers of a wave packet state. The energy of the particle is simply the corresponding value of the Hamiltonian; the density of states in the six-dimensional phase space $(\mathbf{r},\mathbf{k})$ is $(2\pi)^{-3}$, where sums over states are replaced by integrals over phase space. These semiclassical approximations are valid in the limit of large N, as discussed in the Appendix.

In the semiclassical limit, the number density in phase space is

$$w(\mathbf{r},\mathbf{k};T,\mu) = \frac{1}{(2\pi)^3}\,\frac{1}{e^{\beta(\mathcal{H}(\mathbf{r},\hbar\mathbf{k})-\mu)}+1}. \tag{11}$$

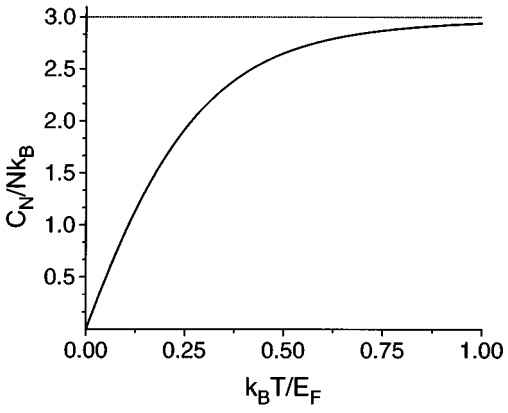

FIG. 2. Heat capacity vs temperature. The heat capacity is scaled by k_BN and the temperature by E_F. The classical result is shown by the dotted line.

The chemical potential is given implicitly by the requirement

$$N=\int d^3\mathbf{r}\, d^3\mathbf{k}\; w(\mathbf{r},\mathbf{k};T,\mu). \tag{12}$$

It follows from the correspondence principle that the Thomas-Fermi calculation of $\mu(T,N)$ using Eq. (12) reproduces the exact result obtained from Eq. (4); this is easily confirmed for the harmonic oscillator, since the two integrals are related by a simple change of variables.

After computing $\mu(T,N)$, it is straightforward to calculate the spatial and momentum distribution functions

$$n(\mathbf{r};T)=\int d^3\mathbf{k}\; w(\mathbf{r},\mathbf{k};T,\mu), \tag{13}$$

$$\tilde{n}(\mathbf{k};T)=\int d^3\mathbf{r}\; w(\mathbf{r},\mathbf{k};T,\mu). \tag{14}$$

VI. SPATIAL DISTRIBUTION AT ZERO TEMPERATURE

At zero temperature, we may define a ''local'' Fermi wave number $k_F(\mathbf{r})$ by

$$\frac{\hbar^2 k_F(\mathbf{r})^2}{2M}+V(\mathbf{r})=E_F, \tag{15}$$

where $V(\mathbf{r})$ is the trap potential. The density $n(\mathbf{r})$ is then simply the volume of the local Fermi sea in k space, multiplied by the density of states $(2\pi)^{-3}$

$$n(\mathbf{r};T=0)=\frac{k_F(\mathbf{r})^3}{6\pi^2}. \tag{16}$$

Note that $n(\mathbf{r})$ vanishes for $\rho>R_F$, where ρ is the effective distance

$$\rho\equiv[x^2+y^2+\lambda^2 z^2]^{1/2}. \tag{17}$$

Combining Eqs. (15) and (16), we obtain (for $\rho\leqslant R_F$)

$$n(\mathbf{r};T=0)=\frac{N\lambda}{R_F^3}\frac{8}{\pi^2}\left[1-\frac{\rho^2}{R_F^2}\right]^{3/2}, \tag{18}$$

which has been derived elsewhere [7,10] by direct summation of harmonic-oscillator eigenstates. The cloud encompasses an ellipsoid with diameter $2R_F$ in the x-y plane, and diameter $2R_F/\lambda$ along the z axis. This aspect ratio is the same as that of a classical gas in the same potential, since the Boltzmann distribution also depends only on ρ: $n_{\text{classical}}(\mathbf{r},T)\sim\exp[-M\omega^2\rho^2/2k_BT]$.

VII. MOMENTUM DISTRIBUTION AT ZERO TEMPERATURE

One way to characterize the state of a trapped gas is to allow a rapid adiabatic expansion and then measure the velocity distribution by time-of-flight spectroscopy [1]. For the degenerate Bose gas, the observed anisotropy of this velocity distribution is dramatic evidence for quantum statistical effects. The semiclassical momentum distribution for a degenerate Fermi gas at zero temperature is simply

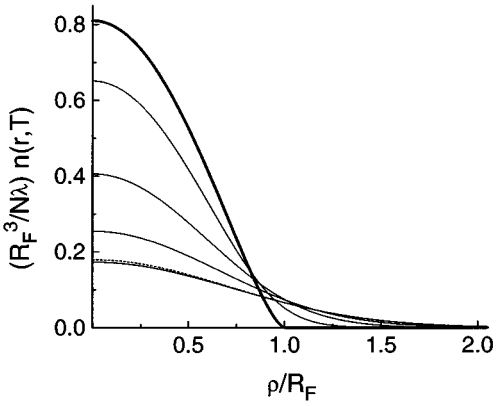

FIG. 3. Universal spatial and momentum density distributions for $k_BT/E_F=0$ (bold), 0.25, 0.5, 0.75, and 1.0. The classical result for $k_BT/E_F=1$ is shown as a dashed line.

$$\tilde{n}(\mathbf{k};T=0)=\frac{1}{(2\pi)^3}\int d^3\mathbf{r}\;\Theta(k_F(\mathbf{r})-|\mathbf{k}|), \tag{19}$$

where $\Theta(k_F(\mathbf{r})-|\mathbf{k}|)$ is the unit step function. The integral (19) is the real-space volume within which the local Fermi wave vector exceeds $|\mathbf{k}|$

$$\tilde{n}(\mathbf{k};T=0)=\frac{N}{K_F^3}\frac{8}{\pi^2}\left[1-\frac{|\mathbf{k}|^2}{K_F^2}\right]^{3/2}, \tag{20}$$

where the maximum occupied wave number K_F was defined in Eq. (7). Note that $k_F(\mathbf{r}=0)=K_F$.

Despite the spatial anisotropy of the trap, the momentum distribution of the degenerate Fermi gas is isotropic. This isotropy is a general feature of trapped Fermi gases, independent of the trap potential [11], since from Eq. (19) we see that $\tilde{n}(\mathbf{k})$ depends only on the magnitude of $\mathbf{k}$.

The spatial and momentum distributions (18) and (20) both have the same functional form, because $\mathcal{H}$ is a quadratic function of both position and momentum. In this sense, the distribution (18) can be viewed as a Fermi sea in real space. If the spring constants of the trap are unequal, then $n(\mathbf{r})$ will be anisotropic. The momentum distribution $\tilde{n}(\mathbf{k})$, however, is always isotropic due to the isotropy of mass. That is, p_x^2, p_y^2, and p_z^2 enter the Hamiltonian with the same coefficient, while x^2, y^2, and z^2 need not.

VIII. NUMERICAL RESULTS

In the semiclassical approximation, the spatial and momentum distributions are easily determined numerically for any temperature as described in Sec. V. As with the chemical potential, an appropriate scaling of these two distributions yields a universal form for all harmonically trapped Fermi gases when plotted versus the scaled variables ρ/R_F and $|\mathbf{k}|/K_F$, respectively.

Figure 3 shows the scaled density versus scaled distance for k_BT/E_F of 0, 0.25, 0.5, 0.75, and 1. At low temperatures, the density is close to its zero-temperature form (bold curve), Eq. (18), with a thin evaporated ''atmosphere'' of thickness $\sim R_F(k_BT/E_F)$ surrounding a degenerate liquid ''core.''

In the classical limit, the density approaches a Gaussian in

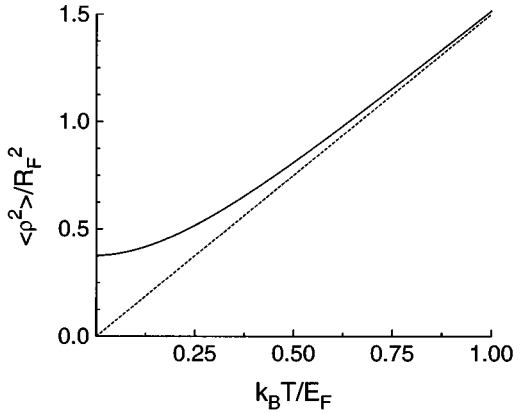

FIG. 4. The mean-square variation of the size of the cloud interpolates between a low-temperature degenerate regime and a high-temperature limit that is well described by the equipartition theorem.

ρ (dashed curve), with a width given by the equipartition theorem: $\langle\rho^2\rangle = 3R_F^2(k_BT/E_F)$. As shown in Fig. 3, this accurately describes the density distribution for $k_BT/E_F = 1$. The evolution of the density profile from its low-temperature Fermi form (18) to the classical limit can be tracked by calculating the mean-square excursion $\langle\rho^2\rangle$, which is shown in Fig. 4 in the dimensionless form $\langle\rho^2\rangle/R_F^2$ vs k_BT/E_F. This is again a universal curve for all harmonically trapped Fermi gases.

At all temperatures, the spatial and momentum distribution have the same form, since momentum and position both enter the single-particle Hamiltonian quadratically. This was seen explicitly for zero temperature in Eqs. (18) and (20). The scaled momentum distribution $K_F^3\tilde{n}(\mathbf{k})/N$ vs $|\mathbf{k}|/K_F$ is therefore also given by Fig. 3. Similarly, Fig. 4 also illustrates the scaled mean-square momentum $\langle\mathbf{k}^2\rangle/K_F^2$ vs k_BT/E_F.

IX. PERTURBATIONS

What happens if the potential is not perfectly harmonic? We may treat $\delta V(\mathbf{r})$ as a perturbation. Here we focus our attention on the $T=0$ case. From Eq. (15), a change in trap potential shifts the local Fermi wave number by

$$\delta k_F(\mathbf{r}) = \frac{M}{\hbar k_F(\mathbf{r})}[\delta E_F - \delta V(\mathbf{r})], \tag{21}$$

where δE_F is the change in Fermi energy. From Eq. (16), the corresponding change in density is

$$\delta n(\mathbf{r}) = \frac{M k_F(\mathbf{r})}{2\pi^2\hbar}[\delta E_F - \delta V(\mathbf{r})], \tag{22}$$

where the Fermi energy is adjusted to make $\int d^3\mathbf{r}\,\delta n(\mathbf{r})$ vanish

$$\delta E_F = \frac{\int d^3\mathbf{r}\ \delta V(\mathbf{r}) k_F(\mathbf{r})}{\int d^3\mathbf{r}\ k_F(\mathbf{r})}. \tag{23}$$

X. COMPARISON WITH THE BOSE GAS

The interacting Bose gases of Refs. [1] and [2] are in the Thomas-Fermi regime [12]. Since the gases remain dilute, two-body scattering may be treated by a δ-function pseudopotential of strength $U = 4\pi\hbar^2 a/M$, where a is the s-wave scattering length. When the dimensionless parameter $UN/(\hbar\omega\lambda\sigma_r^3)$ is large (as is appropriate for the experiments of Refs. [1] and [2]) the density profile of the interacting Bose gas is [12]

$$n_B(\mathbf{r}) = \frac{R_B^2}{2U}\left[1 - \frac{\rho^2}{R_B^2}\right], \tag{24}$$

with maximum radius

$$R_B = \left(\frac{15\lambda UN}{4\pi}\right)^{1/5}. \tag{25}$$

Note that the characteristic radius scales more slowly with the particle number for the Fermi gas ($N^{1/6}$) than for the interacting Bose gas ($N^{1/5}$); similarly, the Fermi energy scales as $N^{1/3}$ while the zero-temperature chemical potential of the Bose gas varies more rapidly, as $N^{2/5}$.

The axial-radial aspect ratio for both classical and degenerate trapped gases is λ, since in all three cases (classical, Fermi, and Bose) the densities are functions of ρ only. The velocity (momentum) distributions, however, can be quite different. For classical and Fermi gases the velocity distribution is isotropic; for a zero-temperature Bose gas, however, $\tilde{n}(\mathbf{k})$ is the square of the Fourier transform of the condensate wave function $\sqrt{n_B(\mathbf{r})}$, which is anisotropic in an asymmetric trap. Note that as N increases, both R_F and R_B increase, but the widths of the respective *momentum* distributions go in opposite directions: K_F increases with N, while the typical momentum of a particle in a trapped Bose condensate decreases with particle number, since $K_B \sim 1/R_B$ by the uncertainty principle.

It is amusing to compare the interatomic repulsion in a Bose gas with the effective repulsion experienced by fermions due to the Pauli exclusion principle [13]. Equating the characteristic Fermi and Bose radii (6) and (25) we see that, crudely speaking, the spatial distribution of a degenerate Fermi gas is mimicked by that of a Bose gas interacting via an effective ''Pauli pseudopotential'' $U_{\text{eff}} \sim E_F(R_F^3/N)$, which is the characteristic energy multiplied by the volume per particle. Equivalently, the effective scattering length brought about by the Pauli principle is $a_{\text{eff}} \sim K_F^{-1}$, i.e., the interparticle spacing. (This is natural, since the interparticle spacing is the only appropriate length in the ideal Fermi gas.) The use of such an effective interaction is limited by the fact that (a) the momentum distributions of the Fermi and Bose gases remain quite different and (b) the gas is not dilute with respect to the exclusion-induced ''interactions'' since $K_F a_{\text{eff}}$ is of order unity.

ACKNOWLEDGMENTS

We thank Mark Kasevich, David Weiss, and Ike Silvera for useful and interesting discussions. This work was supported by the National Science Foundation, under Grant No.

NSF-DMR-91-57414, and the Committee on Research at UC Berkeley. Work at Brandeis was supported by the Sloan Center for Theoretical Neurobiology.

APPENDIX: VALIDITY OF THE SEMICLASSICAL APPROXIMATION

The semiclassical approximation can be safely applied to an inhomogeneous Fermi gas of density $n(\mathbf{r})$ if we can imagine partitioning the system into cells of linear dimension ℓ such that the following two conditions are simultaneously met.

(1) The number of particles in a cell is much greater than unity, so that locally, the gas may be described by a Fermi sea:

$$n(r)\ell^3 \gg 1. \tag{A1}$$

(2) The variation of the trap potential across the cell ($\ell \nabla V$) must be small compared with the local Fermi energy $\hbar^2 k_F(r)^2/2M$, so that within a cell the potential energy is nearly constant. At low temperature, this condition becomes

$$\ell M\omega^2 r \ll \frac{\hbar^2}{2M}[6\pi^2 n(r)]^{2/3}, \tag{A2}$$

where we have used Eq. (16).

Combining Eqs. (A1) and (A2), we see that one can choose a (possibly r dependent) cell size ℓ that simultaneously satisfies these two conditions if the number of particles in a quantum volume is sufficiently large:

$$n(r)\sigma^3 \gg \frac{r}{\sigma}, \tag{A3}$$

where σ is as before the quantum length $(\hbar/M\omega)^{1/2}$ and we have omitted factors of order unity.

At low temperatures, the semiclassical density given by Eq. (18) scales as $N/R_F^3 \sim N^{1/2}/\sigma^3$ near the origin, so the Thomas-Fermi approximation is always self-consistent at the center of the trap for large N. (This can be confirmed at $\mathbf{r}=0$ by direct summation of the squares of the simple harmonic-oscillator eigenfunctions up to energy E_F.) Near the periphery of the cloud, however, the density becomes small, and the approximation fails. It is easy to show that the semiclassical treatment fails within a thin shell at the periphery of the cloud, whose thickness $\delta R \sim 1/K_F \sim \sigma N^{-1/6}$ vanishes in the limit of large N. Within this shell only the exponential tails of a few single-particle states contribute to the density; this is analogous to the corresponding region of the Bose gas [14].

[1] M.H. Anderson, J.R. Ensher, M.R. Matthews, C.E. Weiman, and E.A. Cornell, Science **269**, 198 (1995).

[2] K.B. Davis, M.O. Mewes, M.R. Andrews, N.J. van Druten, D.S. Durfee, D.M. Kurn, and W. Ketterle, Phys. Rev. Lett. **75**, 3969 (1995).

[3] C.C. Bradley, C.A. Sackett, J.J. Tollett, and R.G. Hulet, Phys. Rev. Lett. **75**, 3969 (1995).

[4] H.T.C. Stoof, M. Houbiers, C.A. Sackett, and R.G. Hulet, Phys. Rev. Lett. **76**, 10 (1996).

[5] The treatment of p-wave scattering requires a spatially extended pseudopotential. We estimate the shift in Fermi energy E_F by treating the interparticle interaction as a rectangular pseudopotential of magnitude V_0 and range b. The net strength $(4\pi b^3/3)V_0$ is given by $U=4\pi\hbar^2 a/M$, where a is the s-wave scattering length that would describe collisions of distinguishable particles with the same mass and scattering potential, i.e., neglecting the antisymmetry of the wave function. The range b is roughly 1 nm. In the dilute limit appropriate for trapped gases we have $nb^3 \ll 1$, or equivalently $K_F b \ll 1$. In this long-wavelength limit, the relative shift in Fermi energy is roughly

$$\frac{\delta E_F}{E_F} \sim \frac{UN}{E_F R_F^3}(K_F b)^2,$$

where the factor $(K_F b)^2$ arises from the suppression of the density-density correlation function for spin-polarized fermions at short distances. For the example discussed at the end of Sec. III, for a ^{6}Li gas with $N \sim 10^5$ in the trap of Ref. [1], we find $\delta E_F/E_F \sim 10^{-5} \ll 1$. For the spin-polarized gases of interest, interactions may therefore be neglected.

[6] V.V. Goldman, I.F. Silvera, and A.J. Leggett, Phys. Rev. B **24**, 2870 (1981).

[7] I.F. Silvera and J.T.M. Walraven, J. Appl. Phys. **52**, 2304 (1981).

[8] Note that the trapped gas does not occupy a container of externally fixed size, and so we do not introduce separate constant-volume and constant-pressure specific heats. As the gas is heated, it expands against the harmonic potential, doing work; the specific heat of the harmonically trapped system is therefore expected to be larger than that of a comparable gas in a box at fixed volume. Since the harmonic restoring force grows linearly with the size of the cloud, the effective pressure it exerts will also vary.

[9] L.H. Thomas, Proc. Camb. Philos. Soc. **23**, 542 (1927); E. Fermi, Z. Phys. **48**, 73 (1928).

[10] I.F. Silvera, Physica B **109**, 1499 (1982).

[11] A more familiar case is the ideal Fermi gas in a $L_x \times L_y \times L_z$ rectangular box: while the spatial distribution is clearly anisotropic, the momentum distribution is isotropic, since the density of states in $\mathbf{k}$ space is uniformly $(2\pi)^{-3}$ and the Fermi surface is a sphere.

[12] G. Baym and C.J. Pethick, Phys. Rev. Lett. **76**, 6 (1996).

[13] See, for example, O.O. Tursunov and O.V. Zhirov, Phys. Lett. **222**, 110 (1994); B.L.G. Bakker, M.I. Polikarpov, and A.I. Veselov, Report No. quant-ph/9511009.

[14] S. Stringari, F. Dafolvo, and L. Pitaevskii, Phys. Rev A **54**, 4213 (1996).